

N O T I C E

THIS DOCUMENT HAS BEEN REPRODUCED FROM
MICROFICHE. ALTHOUGH IT IS RECOGNIZED THAT
CERTAIN PORTIONS ARE ILLEGIBLE, IT IS BEING RELEASED
IN THE INTEREST OF MAKING AVAILABLE AS MUCH
INFORMATION AS POSSIBLE

(NASA-TM-80672) AN ALTERNATE ALGORITHM FOR
CORRECTION OF THE SCANNING MULTICHANNEL
MICROWAVE RADIOMETER POLARIZATION RADIANCES
USING NIMBUS-7 OBSERVED DATA (NASA) 27 p
HC A03/MF A01

N80-25762

Unclass
22945

CSCL 14B G3/43



Technical Memorandum 80672

AN ALTERNATE ALGORITHM FOR CORRECTION OF THE SCANNING MULTICHANNEL MICROWAVE RADIOMETER POLARIZATION RADIANCES USING NIMBUS-7 OBSERVED DATA

Per Gloersen
D. J. Cavalieri
Harold V. Soule

APRIL 1980

National Aeronautics and
Space Administration

Goddard Space Flight Center
Greenbelt, Maryland 20771



AN ALTERNATE ALGORITHM FOR CORRECTION OF THE SCANNING
MULTICHANNEL MICROWAVE RADIOMETER POLARIZATION
RADIANCES USING NIMBUS-7 OBSERVED DATA

Per Gloersen
D. J. Cavalieri
Goddard Space Flight Center
Greenbelt, Maryland

Harold V. Soule
OAO Corporation
Beltsville, Maryland

April 1980

GODDARD SPACE FLIGHT CENTER
Greenbelt, Maryland

**AN ALTERNATE ALGORITHM FOR CORRECTION OF THE SCANNING
MULTICHANNEL MICROWAVE RADIOMETER POLARIZATION
RADIANCES USING NIMBUS-7 OBSERVED DATA**

**Per Gloersen
D. J. Cavalieri
Goddard Space Flight Center
Greenbelt, Maryland**

**Harold V. Soule
OAO Corporation
Beltsville, Maryland**

ABSTRACT

This paper discusses the manner in which Nimbus-7 Scanning Multichannel Microwave Radiometer (SMMR) scan radiance data was used to determine its operational characteristics. The predicted SMMR scan radiance was found to be in disagreement at all wavelengths with a large area of average measured ocean radiances. A modified model incorporating a different phase shift for each of the SMMR horizontal and vertical polarization channels was developed and found to provide good data correlation. Additional study will be required to determine the validity and accuracy of this model.

CONTENTS

	<u>Page</u>
ABSTRACT	iii
1.0 INTRODUCTION	1
2.0 RELEVANT SMMR CHARACTERISTICS	1
3.0 ANALYSIS PROCEDURE	2
4.0 OBSERVATIONS	3
5.0 ANALYSIS DETAILS	4
6.0 CONCLUSIONS	8
REFERENCES	9

TABLES

<u>Table</u>	<u>Page</u>
I Regression Values for the 30°-50° South Latitude Ocean Areas (Day)	6
I(a) Regression Values for the 30°-50° South Latitude Ocean Areas (Night).	7

ILLUSTRATIONS

<u>Figure</u>	<u>Page</u>
1 SMMR Sensor System	10
2 Geometric Characteristics of SMMR	11
3 SMMR Multifrequency Feed-Horn Containing Frequency Filtering Polarization Apertures	12
4 Polarization Computed for a Uniformly Emitting Surface, Using the SMMR Hardware Configuration, Compared to the True Radiation from the Earth's Surface	13

ILLUSTRATIONS (Continued)

<u>Figure</u>		<u>Page</u>
5	Southern Hemisphere Ocean Areas Chosen for Basic SMMR Calibration	14
6	SMMR Average Polarization for 6.6GHz	15
7	SMMR Average Polarization for 10.6GHz	16
8	SMMR Average Polarization for 18.0GHz	17
9	SMMR Average Polarization for 21.0GHz	18
10	SMMR Average Polarization for 37.0GHz (1st Half)	19
11	SMMR Average Polarization for 37.0GHz (2nd Half)	20
12	Schematic Indicating the Meaning of the SMMR Orbital Data at 6.6GHz (Day)	21

AN ALTERNATE ALGORITHM FOR CORRECTION OF THE SCANNING MULTICHANNEL MICROWAVE RADIOMETER POLARIZATION RADIANCES USING NIMBUS-7 OBSERVED DATA

1.0 INTRODUCTION

In order to accommodate the weight and volume constraints imposed by the Nimbus-7 spacecraft, it was deemed necessary to design the Scanning Multichannel Microwave Radiometer (N-7/SMMR) in such a way that the multispectral receiving horn part of the antenna remained fixed while the off-axis paraboloid antenna dish scans, (Ref. 1). According to geometric optical theory the orthogonal polarization measured by SMMR should rotate symmetrically with respect to an earth coordinate system.

In this report, the theoretically predicted polarization rotation was tested against N-7/SMMR data acquired in orbit and found to be in disagreement with the observations. In an analysis incorporating a different phase shift into the geometrical polarization rotation model for each of the ten horizontal and vertical polarization N-7/SMMR channels it was found that the modified model matched the data with an accuracy equal to or less than the radiometer noise levels.

Since many uncontrollable parameters are involved in this type of analysis it is highly desirable to make a much more complete analysis to determine the model accuracy. This has not been feasible because reduced data is available for only October/November 1978 and extensive work is required at present to expand the analysis.

2.0 RELEVANT SMMR CHARACTERISTICS

Mounted on the Nimbus-7 satellite, the Scanning Multichannel Microwave Radiometer (SMMR) antenna, shown in Figure 1, scans the earth surface at an incidence angle of 50° with respect to the local vertical as shown in Figure 2(a). The antenna oscillates about the feed horn axis from left to right (-25° to $+25^\circ$) and back again across the plane of the trajectory in the manner shown in Figure 2(b). The multispectral receiving horn shown in Figure 3 is located at

the radiation focal point of the rotating dish antenna. It is fixed in relation to the Nimbus 7 orbit plane. Thus none of the frequency/polarization feed point apertures located in the receiving horn rotate with the antenna.

As a result of this configuration the instrument polarization axis rotate with respect to the earth coordinates and the measured horizontal and vertical polarization values are nominally maximum at some point near the plane of the trajectory. As the antenna angle increases the difference between horizontal and vertical polarization approaches zero as is indicated in Figure 4. Ideally the horizontal and vertical polarization would be equal at about 45° because of the manner in which the SMMR hardware was designed.

If the receiving horn rotated with the antenna or the SMMR antenna orientation were fixed with respect to the Nimbus 7 and the satellite rotated about its vertical axis, for a uniform emitting surface, the difference between the horizontal and vertical polarization would remain fixed throughout a complete rotation as is indicated in Figure 4.

3.0 ANALYSIS PROCEDURE

In order to test the nominal model, earth-located raw radiance data available on the (N-7/SMMR) Antenna Temperature Tape (TAT) product were calibrated using the same temperature transfer algorithm (Ref. 2) incorporated in the CELL tape* production and stored in the TAT format. The calibrated radiance data types are designated TBT's. In addition, a composite TAT was produced by averaging over 8 scan periods and retaining all of the 64 housekeeping words in additional records. This permitted stacking approximately 300 orbits (worth of data) on a single 6250 BPI tape to facilitate the analysis. A composite TBT was produced from the composite TAT.

*Radiance data grouped by cells and bands of various sizes.

Next, a suitable geographical area was selected over which the radiances observed in each of the IFOV's for the 10 SMMR channels would be averaged for the 300 orbits of data stored on the composite TBT. In this way, variations in the TBT's across the swath due to variations in the atmosphere and the surface of the earth were averaged. The resulting artificially produced isotropic surface was used in testing the polarization rotation model.

As is shown in Figure 5, three land-free ocean areas were chosen, all between the latitudes of 30° and 50° South. These were off the west coast of Australia to near the east coast of the South Africa (105° to 40°), from near the west coast of South Africa to near the east coast of South America (10° to 320°) and from near the west coast of South America to some distance off the east coast of New Zealand (275° to 190°). Over these ocean areas the descending and ascending portions of the orbits were kept separate in the averaged values. The time period of the data was for October 25, 1978 (day 298), through November 19, 1978 (day 323), orbits 10 through 369, except for days 321 and 322, which were not available.

4.0 OBSERVATIONS

Figures 6 through 11 show the average of over 2000 data points at each indicated (circle) location for the Vertical (V) and Horizontal (H) polarizations. These points represent data acquired over each integrate-and-dump period (Ref. 1) of the ten N-7/SMMR data channels during the antenna scan. As shown in Figure 2(b) using the spacecraft velocity vector as a reference, the sinusoidal antenna scan is characterized by positive angles to the right and negative angles to the left looking in the forward direction. In all but the 37.0 GHz channels, the instrumental horizontal polarization channels (H) are observed during the right-to-left portion of the scan and the vertical channels (V) during the left-to-right portion. The H&V channels at the 37.0 GHz frequency are observed during both halves of the scan cycle, but the angular positions of the footprints differ slightly since the integrate-and-dump period data are readout at different times (8 milliseconds apart). The south-to-north transversals of the three selected ocean areas were

labeled day and the north-to-south portions of the orbit, night in accordance with the sun synchronous Nimbus-7 orbit.

It will be noted that the points in Figures 6 through 11 lie along the proposed theoretical curve with the minimum (H) or maximum (V) generally not at the center scan position. Theoretically they should lie on the SMMR physical velocity vector at zero scan angle ($\theta = 0^\circ$) but in some cases they are not even on the same side of this reference. This was not expected on the basis of the SMMR design and antenna range tests. The typical physical meaning of the offset values given in Table I and shown in Figure 6 for the 6.6 GHz day measurements is illustrated in Figure 12.

5.0 ANALYSIS DETAILS

The polarized radiation components, H and V, emitted by the earth's surface were assumed to be independent and therefore individually resolved along the axis of the instrument polarizations. Designating the radiance received in the horizontal channel of the instrument as P, the vertical as S, and the radiances from the earth as H and V respectively, the optical model predicts for the signal amplitudes, at a given scan angle:

$$\begin{aligned} P^{1/2} &= H^{1/2} \cos \theta + V^{1/2} \sin \theta \\ S^{1/2} &= H^{1/2} \sin \theta + V^{1/2} \cos \theta \end{aligned} \quad (1)$$

Because of the assumed independence of H and V, the received radiance is given by:

$$\begin{aligned} P &= H \cos^2 \theta + V \sin^2 \theta \\ S &= H \sin^2 \theta + V \cos^2 \theta \end{aligned} \quad (2)$$

Let us assume that the data in Figures 7-12 can be fitted by a function of the form:

$$\begin{aligned} P &= H \cos^2(\theta + \delta_H) + V \sin^2(\theta + \delta_H) \\ S &= H \sin^2(\theta + \delta_V) + V \cos^2(\theta + \delta_V) \end{aligned} \quad (3)$$

where δ_H and δ_V represent the different positions of the minimums and maximums observed in the radiance data vs the scan position. Equation (3) may also be written as:

$$\begin{aligned}
 P &= 1/2(V + H) - 1/2(V - H) \cos 2\delta_H \cos 2\theta + 1/2(V + H) \sin 2\delta_H \sin 2\theta \\
 &= P_0 + P_1 \cos 2\theta + P_2 \sin 2\theta \\
 S &= 1/2(V + H) + 1/2(V - H) \cos 2\delta_V \cos 2\theta - 1/2(V - H) \sin 2\delta_V \sin 2\theta \\
 &= S_0 + S_1 \cos 2\theta + S_2 \sin 2\theta
 \end{aligned} \tag{4}$$

$\cos 2\theta$ and $\sin 2\theta$ can be treated as linear variables. A multiple linear regression of the observations with respect to those variables to obtain values for S_0 , S_1 , S_2 , P_0 , P_1 , and P_2 was performed.

From the coefficients, we obtained:

$$\begin{aligned}
 \delta_H &= 1/2 \text{ ATN } (-P_2/P_1) \\
 \delta_V &= 1/2 \text{ ATN } (-S_2/S_1) \\
 (V - H)_H &= -2P_1 \text{ SEC } (2\delta_H) \\
 (V - H)_V &= 2S_1 \text{ SEC } (2\delta_V) \\
 1/2(V + H)_H &= P_0 \\
 1/2(V + H)_V &= S_0
 \end{aligned} \tag{5}$$

Summarizing the above parameter definitions:

H = Horizontal (H) polarization inflection point value

V = Vertical (V) polarization inflection point value

θ = Antenna position angle

δ = Computed displacement of the average measured (H) or (V) inflection points with respect to the zero antenna angular position

P = Computed SMMR (H) value as a function of θ

S = Computed (V) value as a function of θ

Σ = Standard estimated temperature error (K) (in Table I)

In Table I, the regression results in terms of equation (5) are presented, along with the standard error in the fit of the curves to the radiance values, (Σ). The solid curves shown in

Table I
Regression Values for the 30-50 South Latitude Ocean Areas (Day)

Wavelength Parameters	6.6 GHz		10.7 GHz		18.0 GHz		21.0 GHz		37.0 GHz	
	H	V	H	V	H	V	H	V	H	V
Phase-Angle δ	4.52	-2.79	0.99	0.44	-2.60	1.35	-1.75	10.78	0.47	-0.22*
(V - H)	+44.45	54.82	+49.43	59.14	+45.02	57.10	+35.72	46.89	+41.29	47.56*
Offset Constant 1/2 (V + H)	109.24	115.98	115.10	117.83	126.69	126.91	171.89	160.34	168.39	169.74*
Standard Estimated Error Σ (Kelvins)	0.09	0.18	0.09	0.14	0.17	0.11	0.17	0.11	0.15	0.10*
									0.21	0.08**

*1st half

**2nd half

Table I (a)
Regression Values for the 30-50 South Latitude Ocean Areas (Night)

Wavelength Parameters	6.6 GHz		10.7 GHz		18.0 GHz		21.0 GHz		37.0 GHz	
	H	V	H	V	H	V	H	V	H	V
Phase-Angle δ	+5.51	-3.15	1.98	0.37	-1.25	-1.07	-0.38	+10.57	1.21	-0.19*
(V - H)	+46.26	51.87	+50.61	57.02	+47.18	56.87	+35.72	47.78	+40.94	47.62*
Offset Constant $1/2 (V + H)$	108.27	116.06	116.04	119.09	125.66	125.72	170.84	159.84	168.65	170.67*
Standard Estimated Error Σ (Kelvins)	0.12	0.14	0.12	0.11	0.18	0.14	0.20	0.13	0.23	0.19*
									0.19	0.17**

*1st half

**2nd half

Figures 6-11 were produced using the equations in (3) together with the regression results given in Table I.

6.0 CONCLUSIONS

The excellent fit of the theoretical curves to the data as illustrated in Figures 6 through 11 suggests that the modified optical model for the polarization rotation is correct. As a consequence, we conclude that not only do the P and S polarization directions of the N-7/SMMR not line up with the H and V components from the earth at the center scan position, but also that the P and S directions are not orthogonal. Data phase angles on the order of 5° at 6.6 GHz and 11° at 21 GHz are well outside of manufacturing and range measurement tolerances, estimated as better than 0.5° . Nominal data orthogonality and alignment with H and V at SMMR antenna angle $\theta = 0^\circ$ had been specified.

The reasons for such a discrepancy are presently under investigation, and may be related to the addition of the waveguides and radio frequency switches (See Reference 1) behind the multi-frequency receiving horn after the antenna range measurements were made. Part of the investigation will include field observations using the N-7/SMMR engineering model, upon completion of instrument modifications now in progress. Such observations will help settle the question of whether the observed discrepancies are a fundamental property of the N-7/SMMR or represent a failure mode after installation on the spacecraft.

It will be noted that the values for (V-I) derived for the P and S shown in Table I do not agree precisely with each other for a given SMMR frequency. This is attributed to the preliminary nature of the absolute radiance calibration represented on the TBT's, which have not yet been adjusted to conform with known earth targets. It is our opinion that to a first order the δ_H and δ_V herein determined are invariant with respect to the absolute calibration errors. The effects of time and location of the observations will require considerable additional investigation.

In view of the excellent fit of the theoretical curves to the data, it is feasible to utilize the following algorithm, derived from equation (3), to correct for polarization rotation:

$$\begin{aligned} H &= \alpha_V P + (1-\alpha_V) S \\ V &= (1-\alpha_H) P + \alpha_H S \end{aligned} \tag{6}$$

where: $\alpha_V = (1-\sin^2(\theta + \delta_V)) / (1-\sin^2(\theta + \delta_H) - \sin^2(\theta + \delta_V))$

and: $\alpha_H = (1-\sin^2(\theta + \delta_H)) / (1-\sin^2(\theta + \delta_H) - \sin^2(\theta + \delta_V))$

Note that only values for δ_H and δ_V need be stored; observed values (interpolated along track and cross-track as required) are used for P and S.

It should be noted that there are a number of parameters affecting the averaged SMMR data which are dependent upon the weather and other uncontrollable factors. It therefore will be essential to examine in some detail other time periods and compare the results with those determined in this analysis. Only when this data becomes available can the accuracy of this analysis be fully determined.

REFERENCES

1. Gloersen, Per and Frank T. Barath, (1977), "A Scanning Multichannel Microwave Radiometer for Nimbus-G and Seasat A," IEEE J of Oceanic Engr., Vol. OE-2, No. 2, pg. 172, (April 1977).
2. Gloersen, Per and J. Stacey, (1979), "Prelaunch Calibration Report Nimbus 7 SMMR Instrument," Jet Propulsion Lab., Cal Inst. of Tech., Pasadena, Calif.

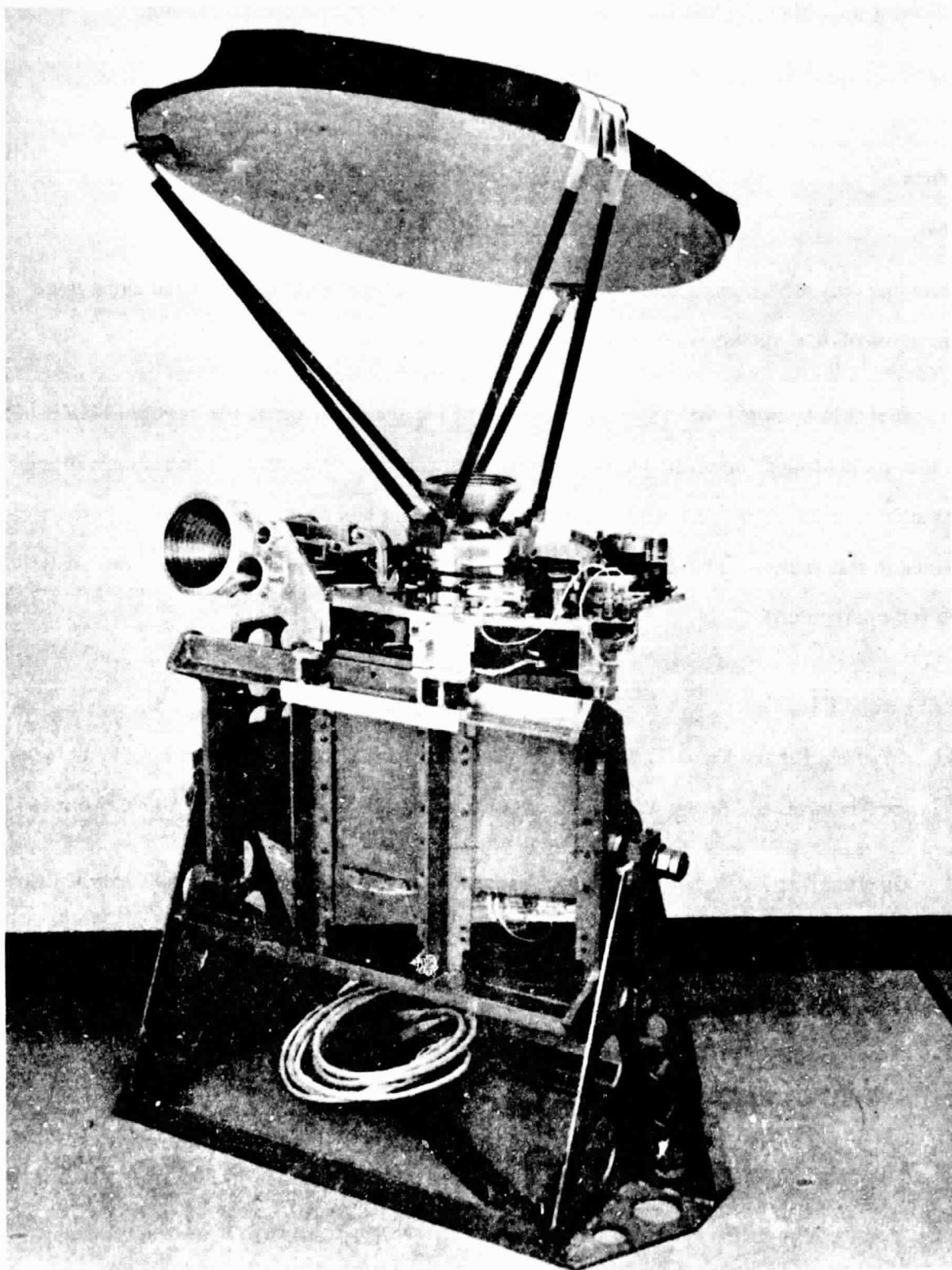


Figure 1. SMMR Sensor System.

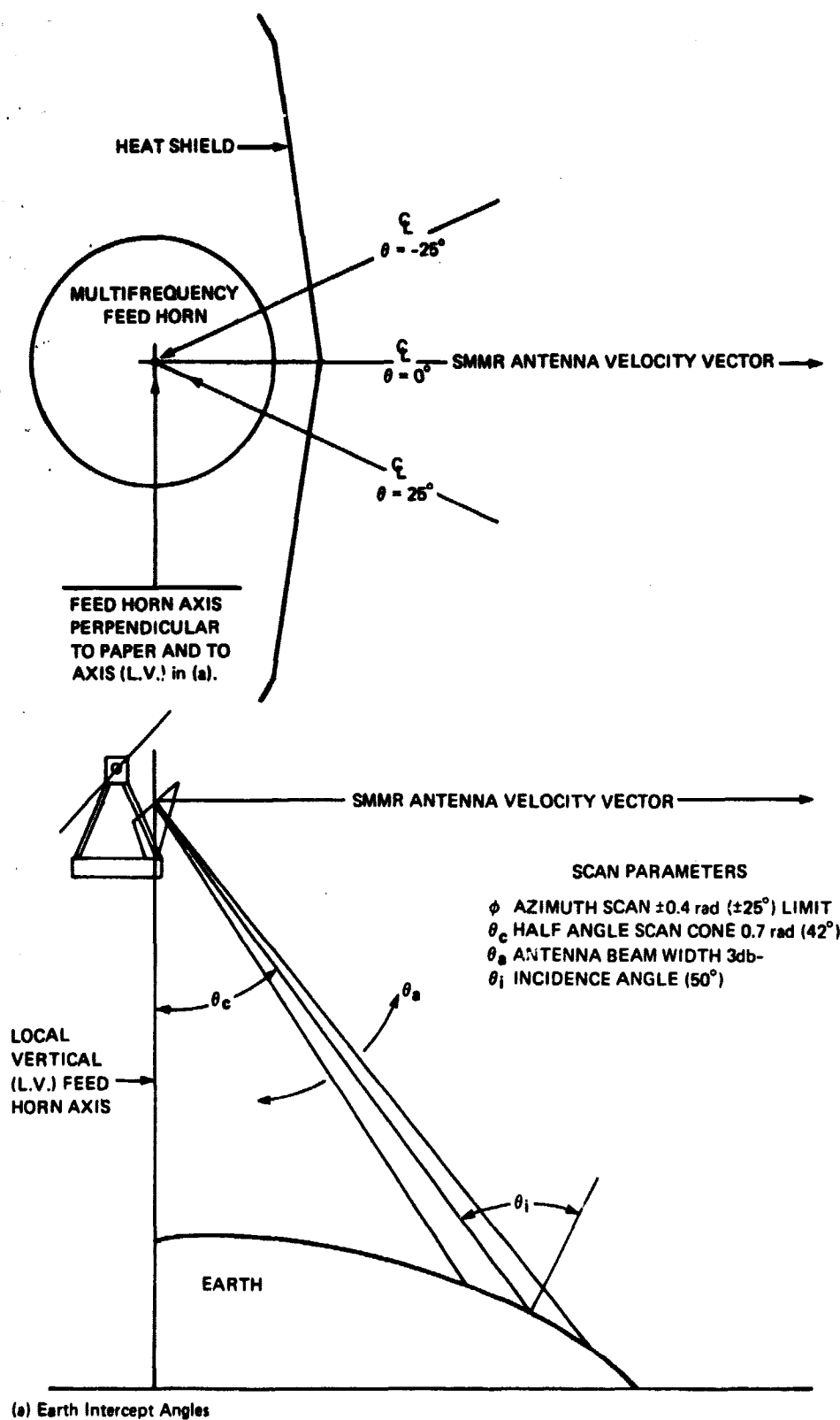


Figure 2. Geometric characteristics of SMMR.

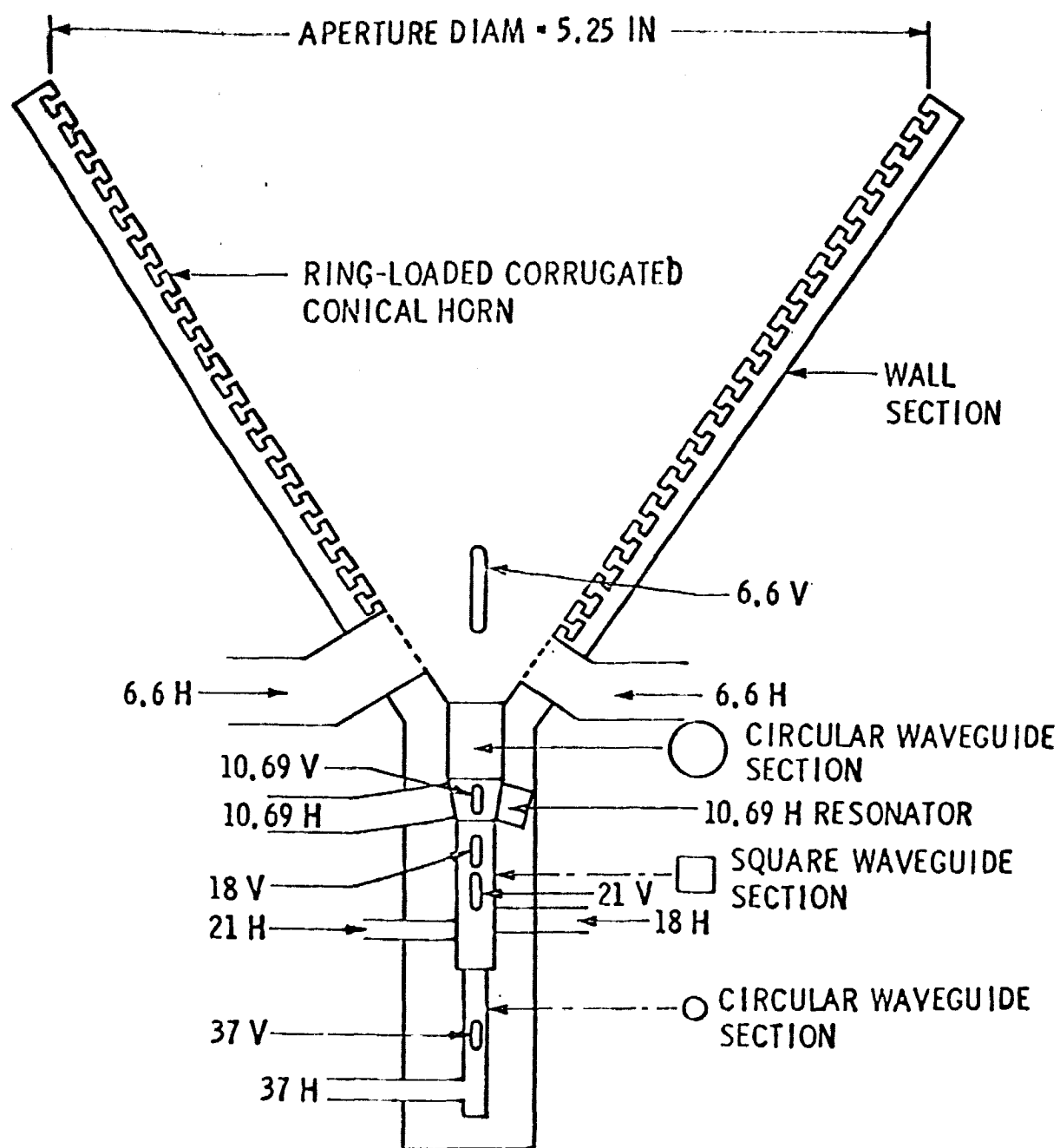


Figure 3. SMMR multifrequency feed-horn containing frequency filtering polarization apertures.

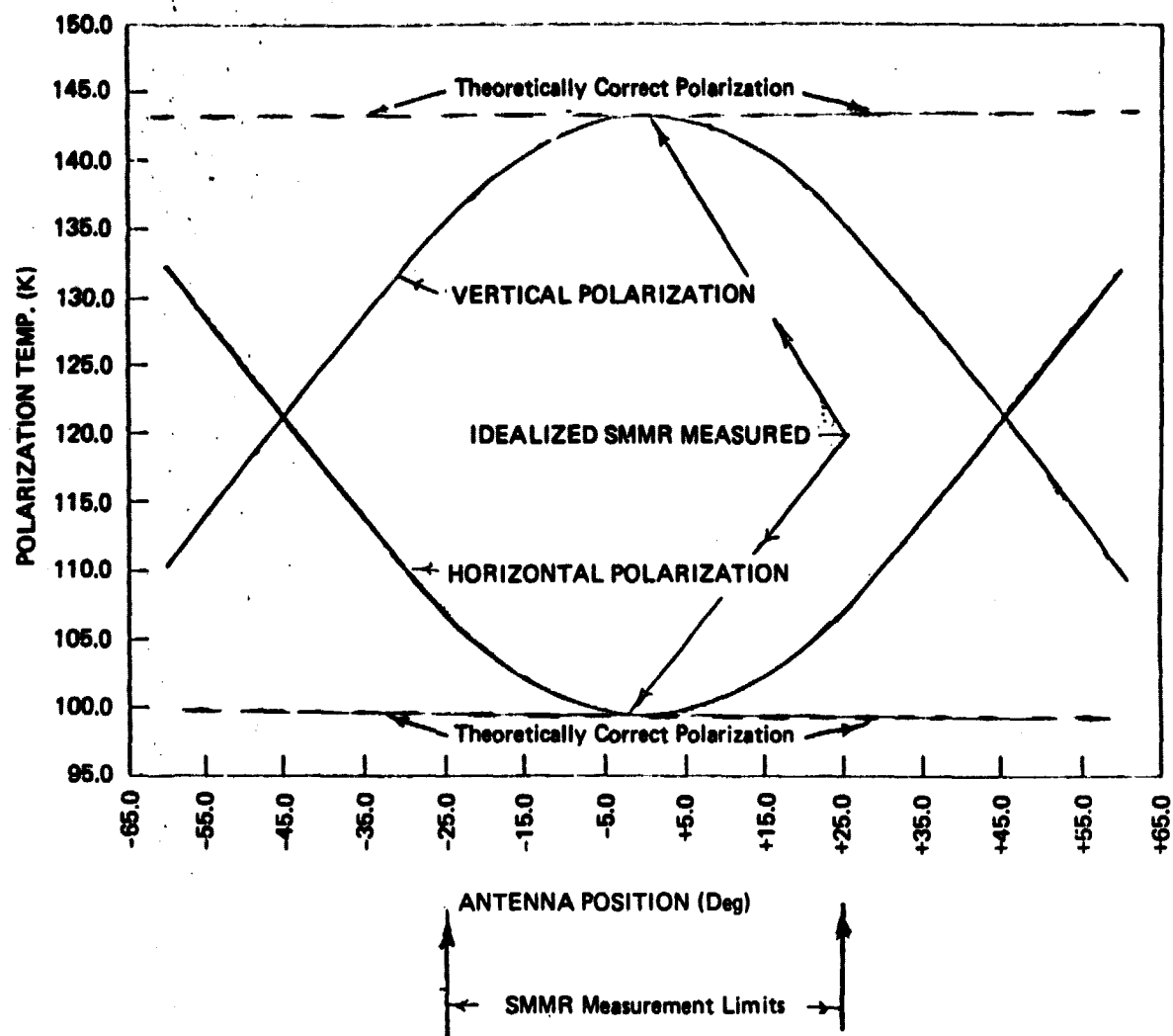


Figure 4. Polarization computed for a uniformly emitting surface, using the SMMR hardware configuration, compared to the true radiation from the earth's surface.

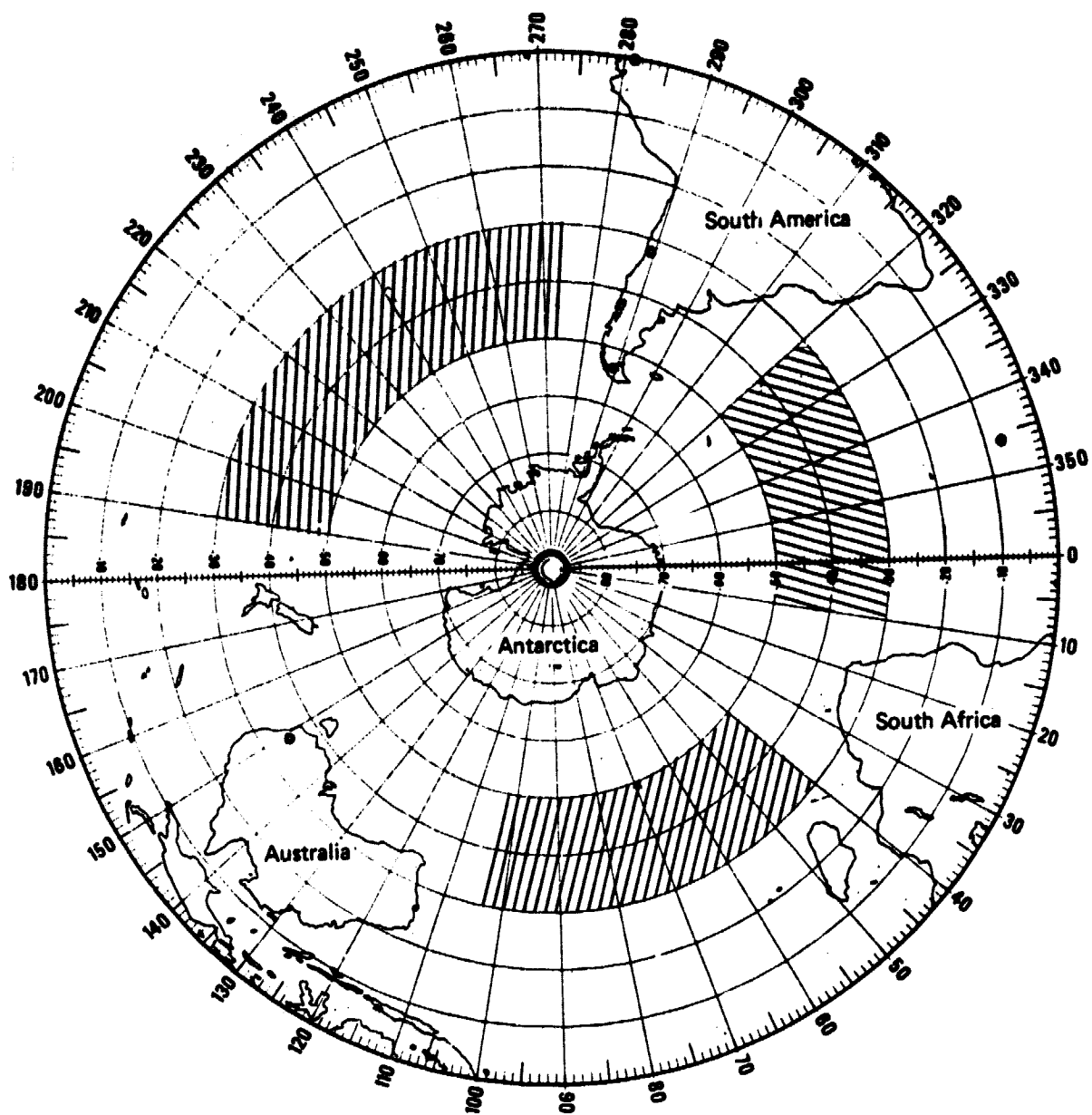
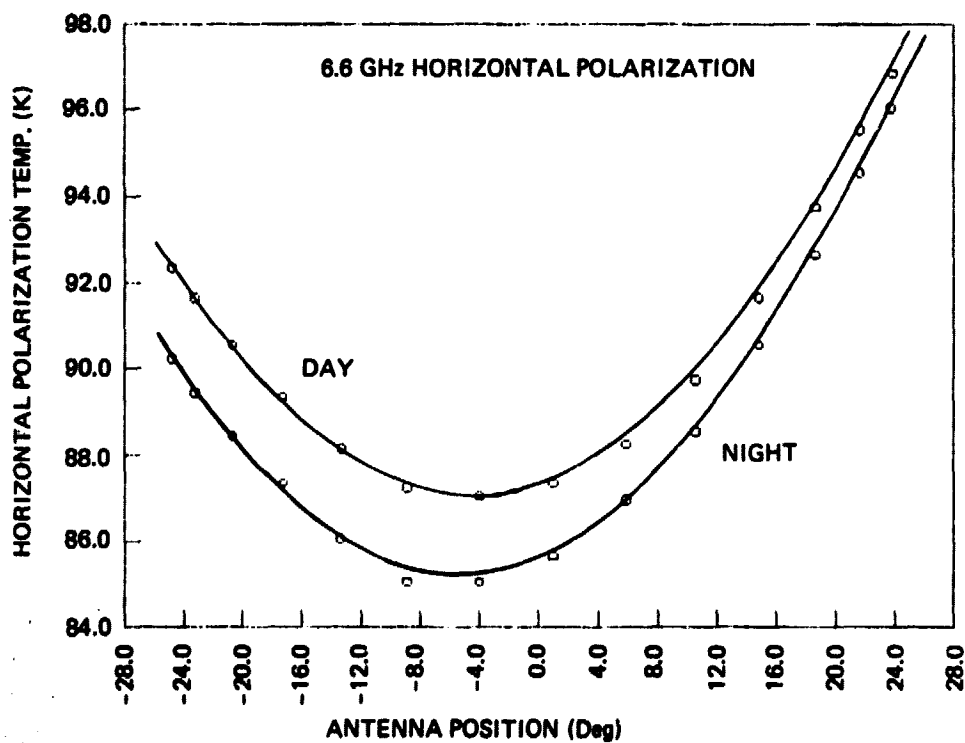
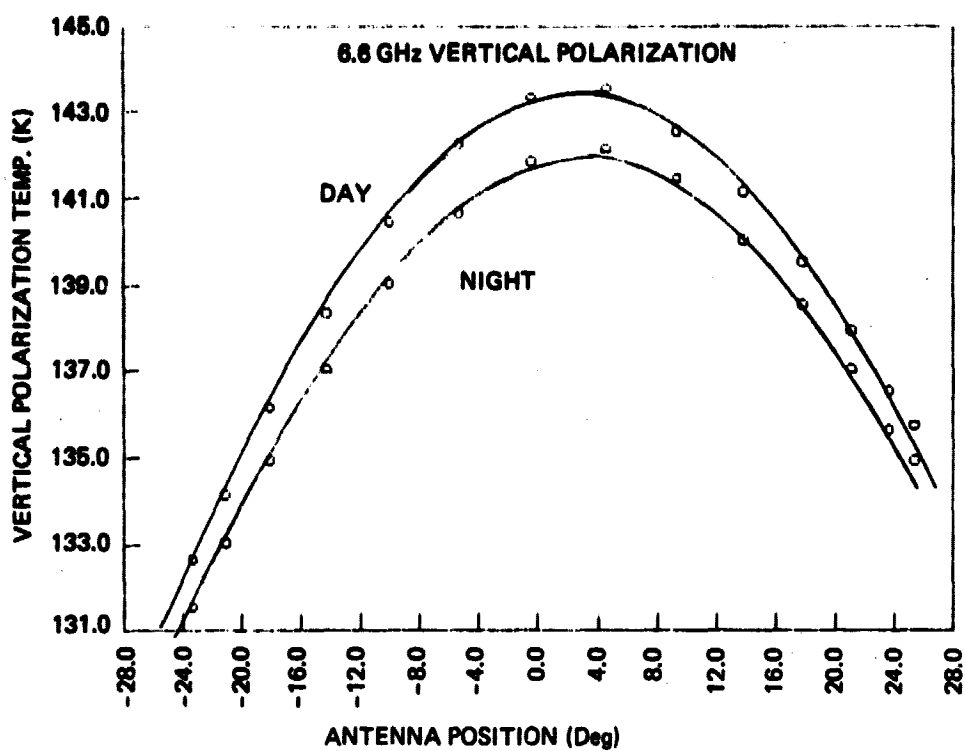
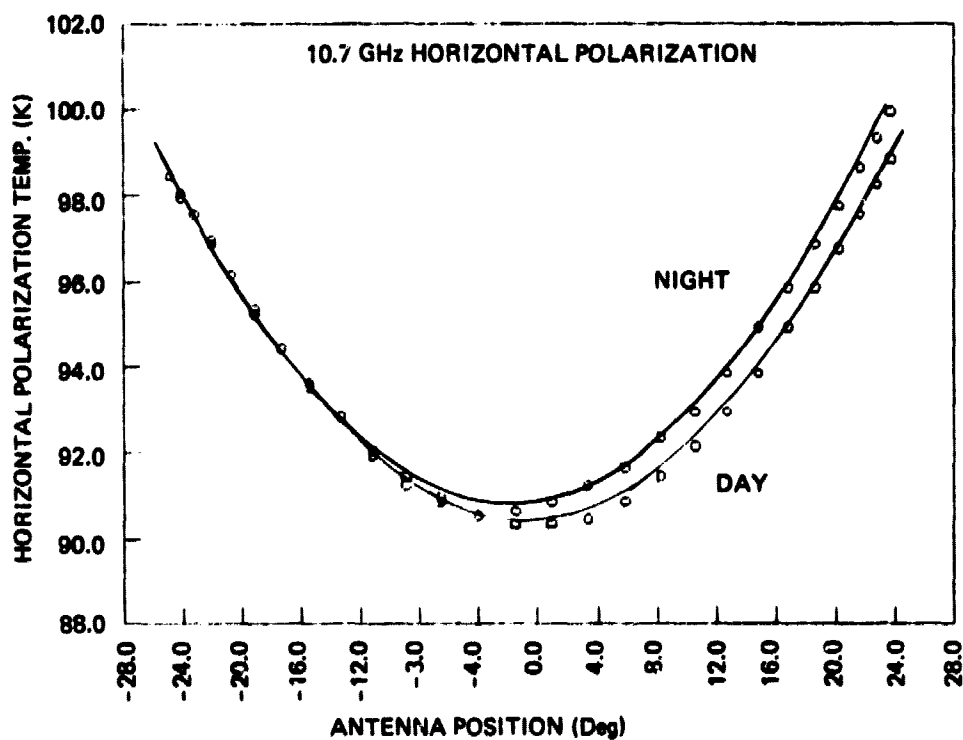
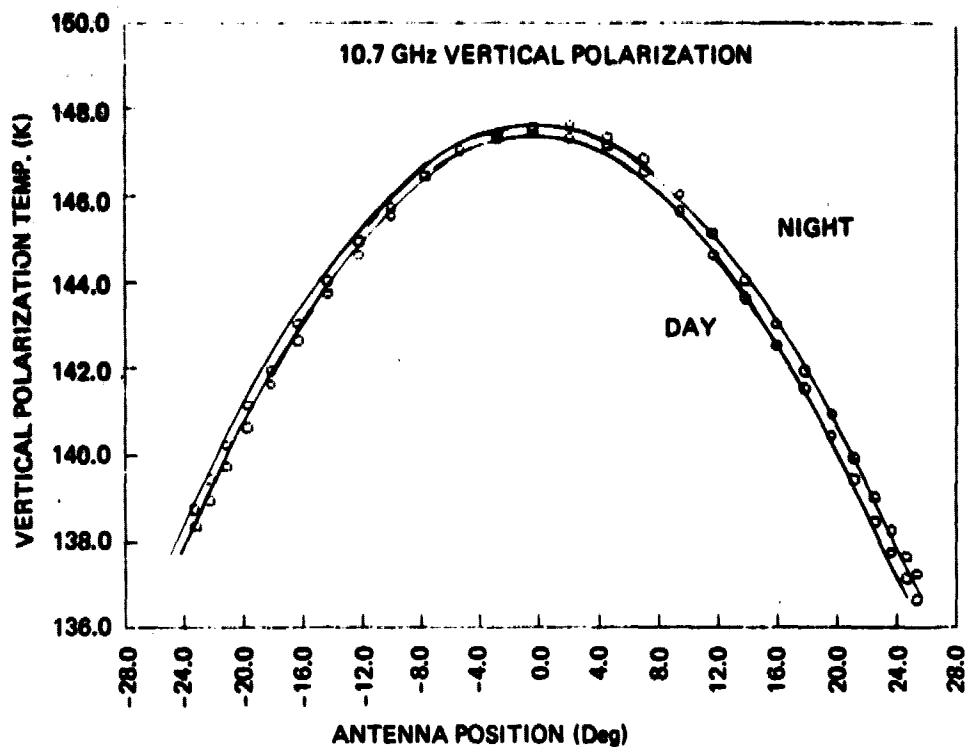


Figure 5. Southern hemisphere ocean areas chosen for basic SMMR calibration.



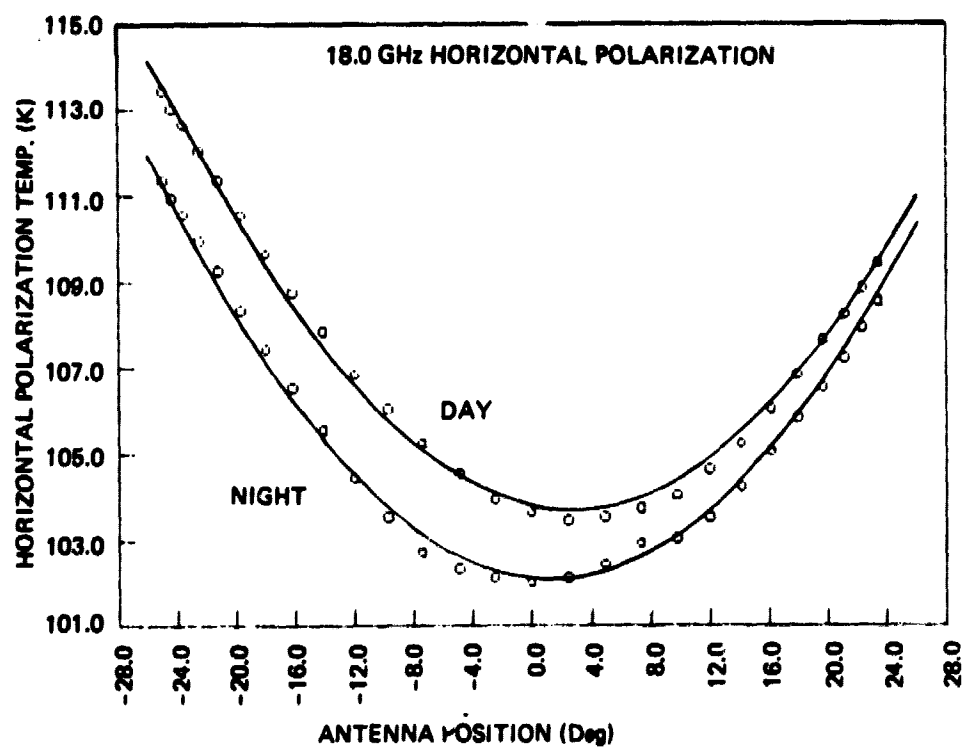
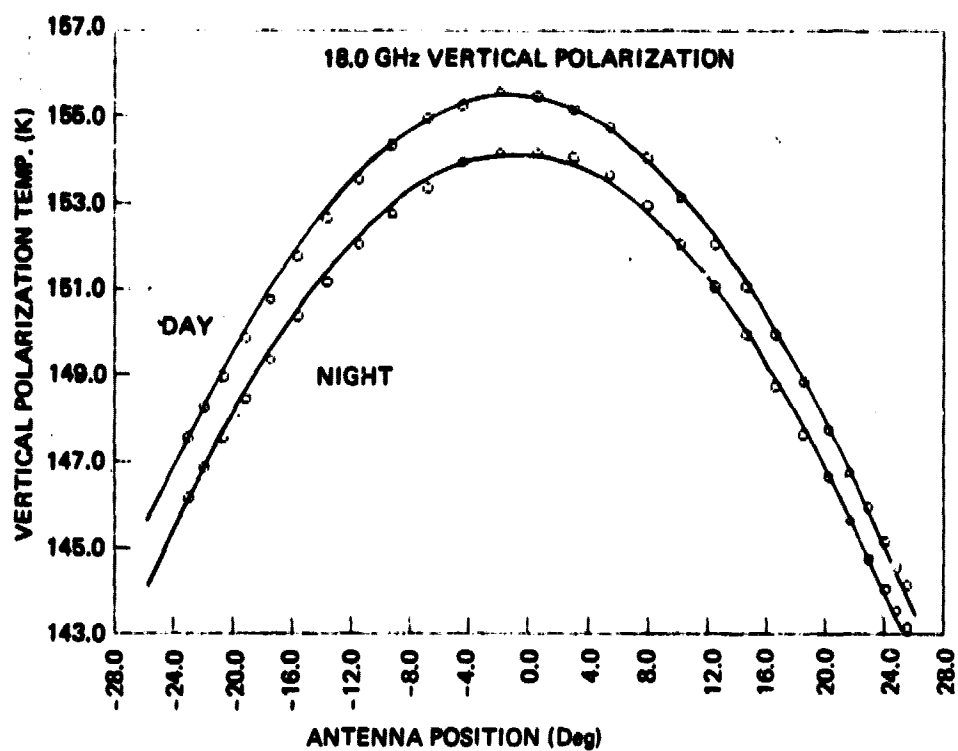
SMMR Ave. Polar. for 3 Southern Ocean Areas - Oct, Nov, '78 (~340 Orb)

Figure 6.



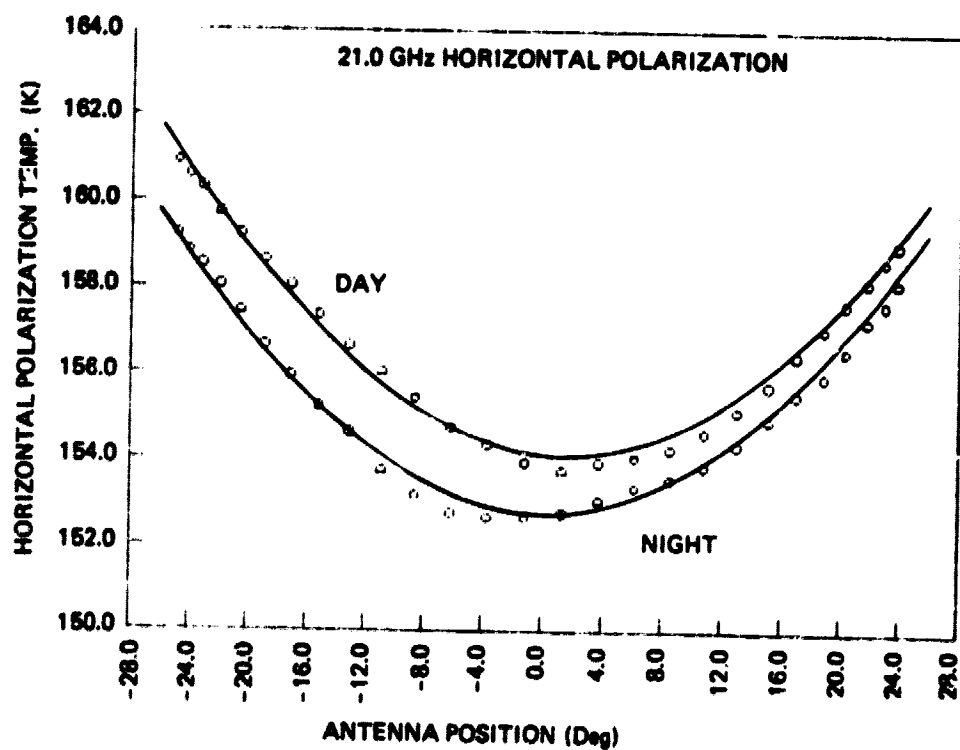
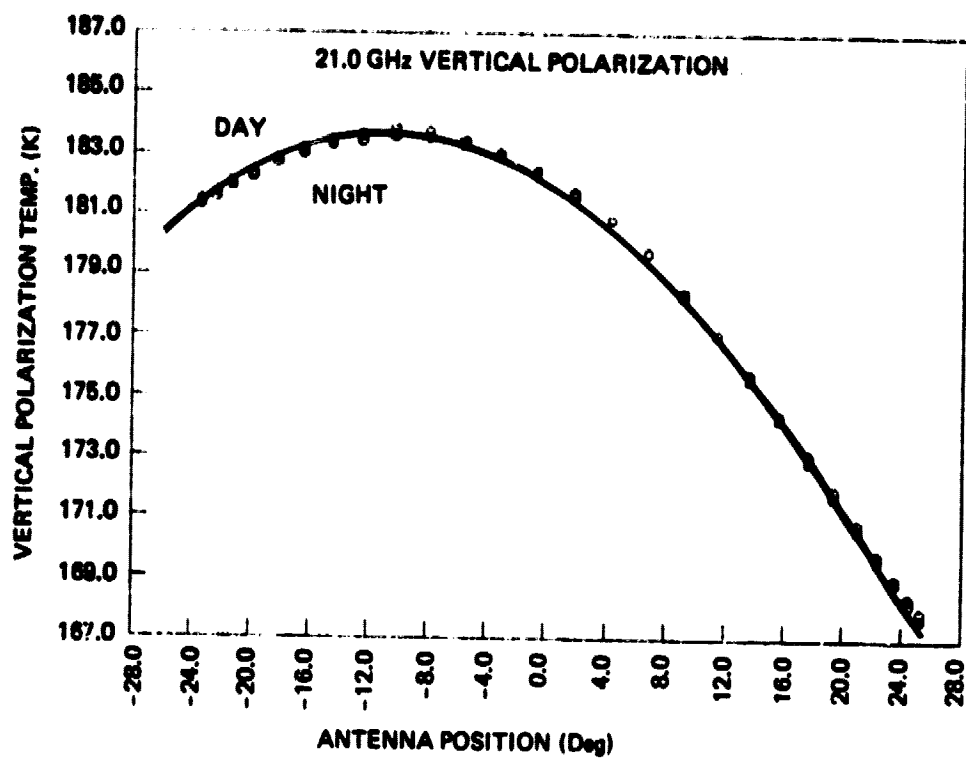
SMMR Ave. Polar. for 3 Southern Ocean Areas - Oct, Nov, '78 (~340 Orb)

Figure 7.



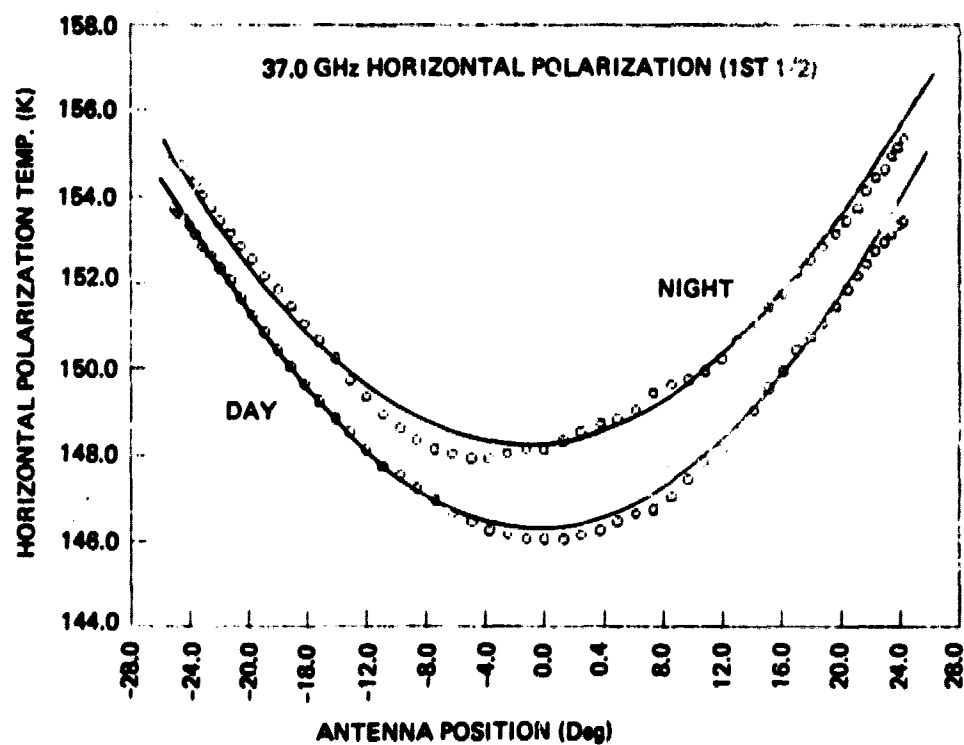
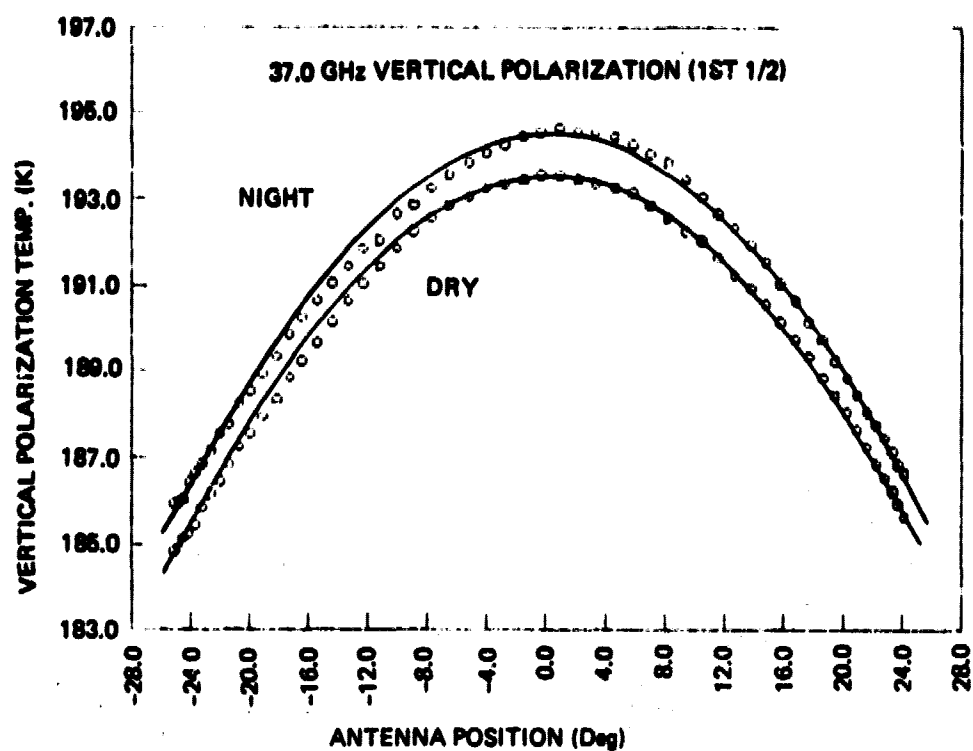
SMMR Ave. Polar. for 3 Southern Ocean Areas - Oct, Nov, '78 (~340 Orb)

Figure 8



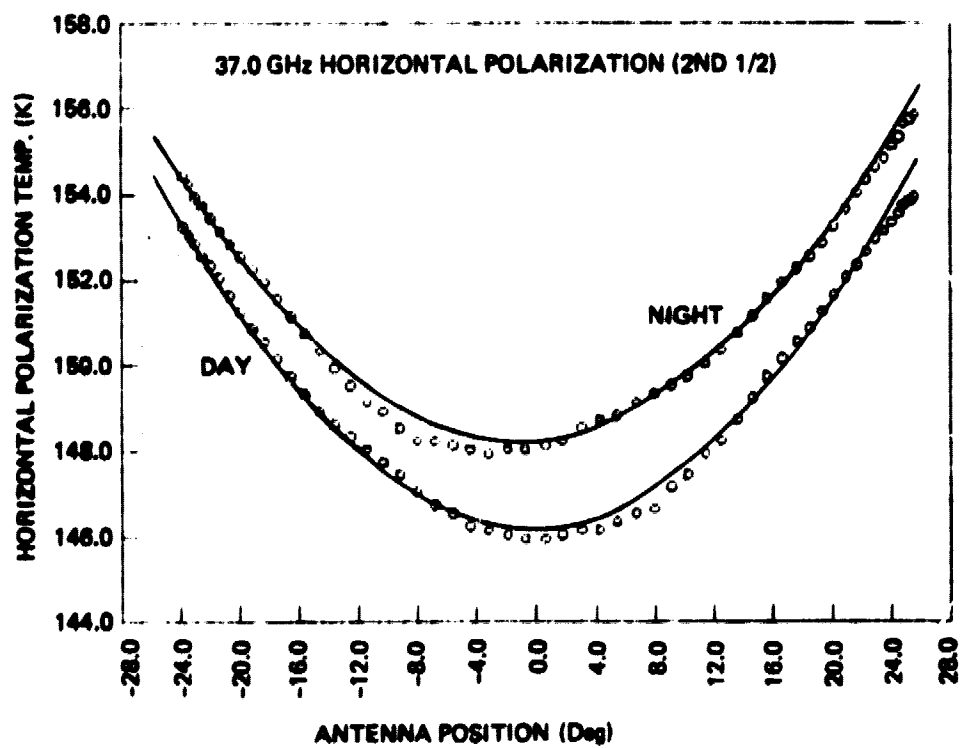
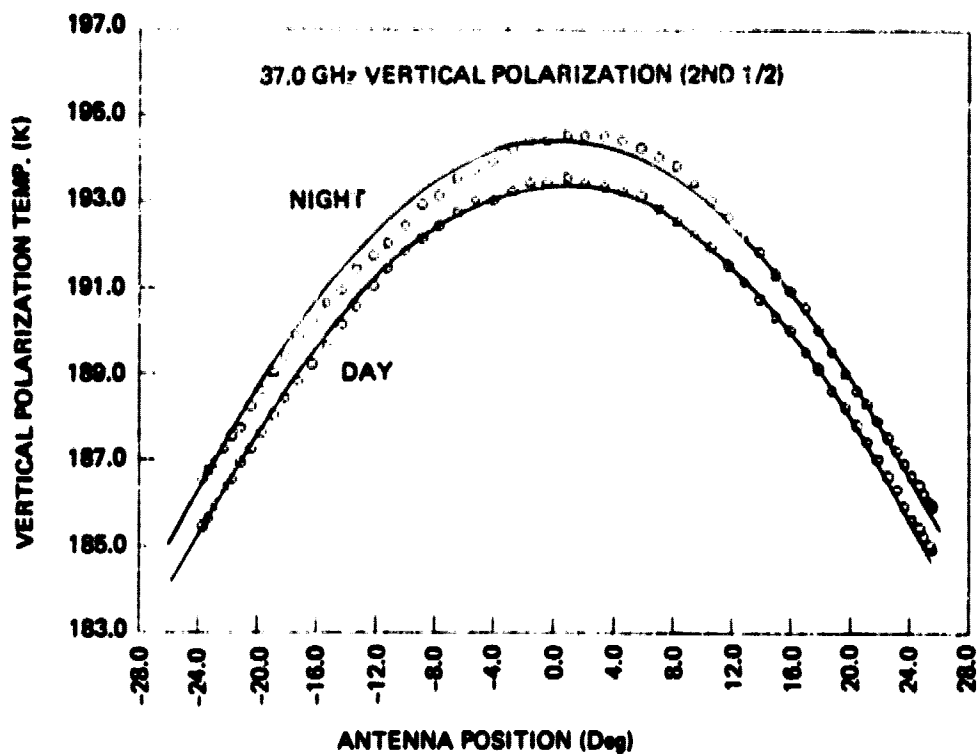
SMMR Ave. Polar. for 3 Southern Ocean Areas - Oct, Nov, '78 (~340 Orb)

Figure 9



SMMR Ave. Polar. for 3 Southern Ocean Areas - Oct, Nov, '78 (~340 Orb)

Figure 10



SMMR Ave. Polar. for 3 Southern Ocean Areas - Oct, Nov, '78 (~340 Orb)

Figure 11

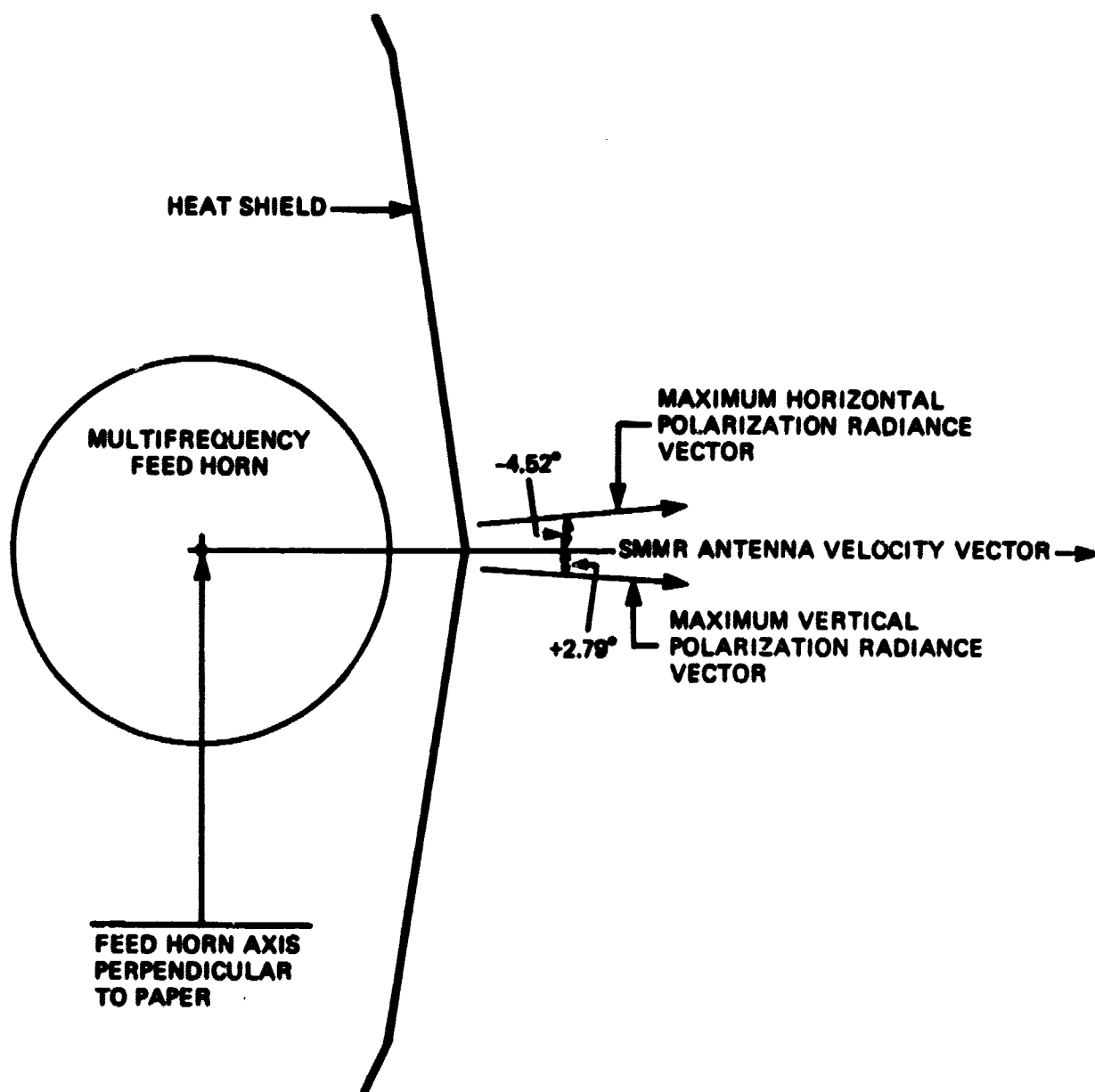


Figure 12. Schematic indicating the meaning of the SMMR orbital data at 6.6GHz (day).

BIBLIOGRAPHIC DATA SHEET

1. Report No. TM 80672	2. Government Accession No.	3. Recipient's Catalog No.	
4. Title and Subtitle An Alternate Algorithm for Correction of the Scanning Multichannel Microwave Radiometer Polarization Radiances Using Nimbus-7 Observed Data		5. Report Date April 1980	
		6. Performing Organization Code 913.0	
7. Author(s) Per Gloersen, D.J. Cavalieri and Harold V. Soule		8. Performing Organization Report No.	
9. Performing Organization Name and Address Goddard Space Flight Center Greenbelt, Maryland		10. Work Unit No.	
		11. Contract or Grant No.	
		13. Type of Report and Period Covered Technical Paper	
12. Sponsoring Agency Name and Address Goddard Space Flight Center Greenbelt, Maryland		14. Sponsoring Agency Code NASA/Goddard	
15. Supplementary Notes			
16. Abstract This paper discusses the manner in which Nimbus-7 Scanning Multichannel Microwave Radiometer (SMMR) scan radiance data was used to determine its operational characteristics. The predicted SMMR scan radiance was found to be in disagreement at all wavelengths with a large area of average measured ocean radiances. A modified model incorporating a different phase shift for each of the SMMR horizontal and vertical polarization channels was developed and found to provide good data correlation. Additional study will be required to determine the validity and accuracy of this model.			
17. Key Words (Selected by Author(s)) Microwave Radiometer SMMR Orbital Polarization Calibration Average Ocean Microwave Radiances		18. Distribution Statement	
19. Security Classif. (of this report) Unclassified	20. Security Classif. (of this page) Unclassified	21. No. of Pages 21	22. Price*